

Kinematic and Dynamic Characteristics of Pulsating Flow in 180° Tube

Tin-Kan Hung^{1,*}, Ruei-Hung Kuo² and Cheng-Hsien Chiang³

¹Department of Bioengineering, University of Pittsburgh, 4200 Fifth Ave, Pittsburgh, PA 15260, USA

²Department of Aeronautics and Astronautics, National Cheng Kung University, Tainan

³Department of Biomedical Engineering, National Cheng Kung University, Tainan

*Corresponding Author: Tin-Kan Hung. Email: tkhung@pitt.edu

Received: 04 July 2019; Accepted: 09 July 2019.

Abstract: Kinematic and dynamic characteristics of pulsating flow in a model of human aortic arch are obtained by a computational analysis. Three-dimensional flow processes are summarized by pressure distributions on the symmetric plane together with velocity and pressure contours on a few cross sections for systolic acceleration and deceleration. Without considering the effects of aortic tapering and the carotid arteries, the development of tubular boundary layer with centrifugal forces and pulsation are also analyzed for flow separation and backflow during systolic deceleration.

Keywords: Aortic arch; curve tube; pressure; pulsating flow; vortex

1 Introduction

The complexity of pulsating flow in the aortic arch involves the effects of branching flows and geometric variations and rheological properties of the aorta. The computational fluid dynamic (CFD) analysis is useful and effective for hemodynamics. As human cardiac vascular system is capable of responding to various physiological conditions, understanding of the kinematic and dynamic characteristics in an 180° curved tube with a straight segment in the downstream could provide the fundamentals for cardiovascular dynamics and biomedical engineering application before modeling more sophisticated physical and physiological flow conditions. The present study is oriented towards the main characteristics of the rapidly accelerated and decelerated blood flow in the simplified aortic arch.

2 Methodology

In this study, a computational fluid dynamic (CFD) analysis is conducted for pulsating blood flow in an aortic model with a prescribed inlet velocity, $V_0(t)$, which can be expressed as the instantaneous Reynolds number, $\mathbf{Re}(t) = \rho DV_0/\mu$ in which D is the tube diameter, ρ the blood density and μ the dynamic viscosity. Computation of pressure field requires a reference pressure at the downstream end section. It is based on the pressure pulse in Professor Y. C. Fung's book [1]. The 3D velocity and pressure fields during a rapid acceleration and deceleration cannot be obtained without the CFD analysis. The finite volume method of an arbitrary Lagrangian-Eulerian (ALE) formulation of the Navier-Stokes equations is used [2]. For a volume V and surface S with velocity \vec{v}_b on the boundary and the unit normal vector \vec{n} , the integral form of the continuity equation is

$$\frac{\partial}{\partial t} \int_V \rho dV + \int_S \rho (\vec{v} - \vec{v}_b) \cdot \vec{n} dS = 0 \quad (1)$$

The momentum equation is



$$\int_V \frac{\partial}{\partial t} (\rho \vec{v}) dV + \int_S \rho \vec{v} (\vec{v} - \vec{v}_b) \cdot \vec{n} dS = - \int_S p \mathbf{I} \cdot \vec{n} dS + \int_S \boldsymbol{\tau} \cdot \vec{n} dS \quad (2)$$

in which p is the pressure, \mathbf{I} the unit tensor, and $\boldsymbol{\tau}$ the viscous stress tensor. The numerical solutions are obtained by using 2704 cells for each of 247 cross sections.

3 Results and Discussion

For flow computation with a prescribed inlet velocity $V_o(t)$ and $P_b(t)$ on the outlet shown in Fig. 1, the initial flow field is under a hydrostatic condition. Since the velocity distribution at the inlet is not known a priori, one can consider the transient boundary layer is developed from this section. This simplification is necessary when the flow through the sinuses of Valsalva is not included in the 3D computation. The inlet velocity is, therefore, only a function of time. Also shown in the figure is the geometry of the curved tube with the radius of curvature $R = 1.32D$.

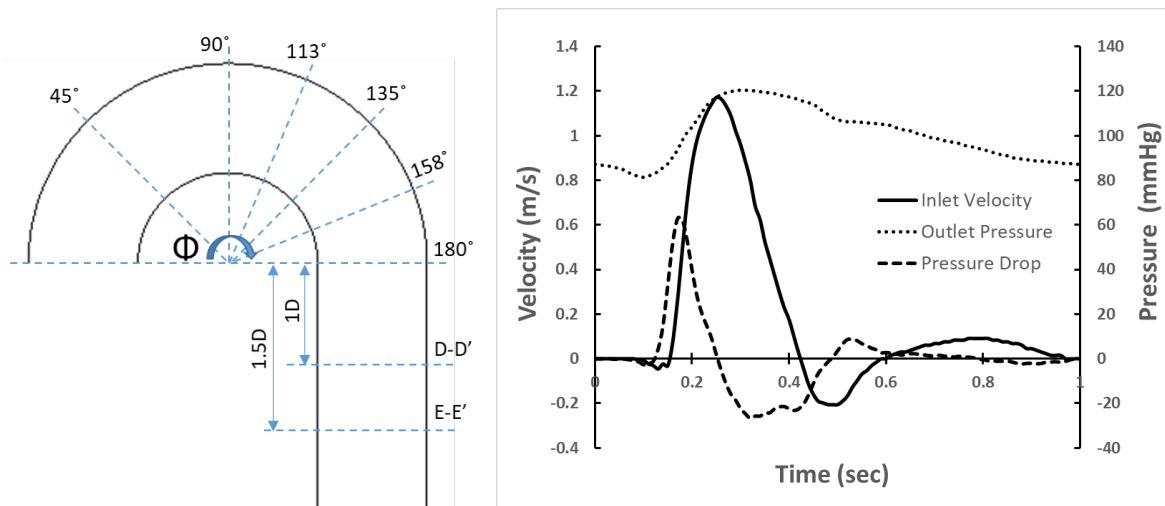


Figure 1: Schematic sketch of the curved tube and the prescribed inlet velocity and outlet pressure

The results in Fig. 2 include pressure contours on the symmetric plane for $Re = 5104$ and 12097 , the longitudinal velocity and pressure distributions on a cross section $\phi = 113^\circ$. For $Re = 5104$, the velocity and pressure are dominated by the rapid boundary layer development from the onset systole (at $t = 0.15$ sec) to $t = 0.20$ second. The curvature effect is coupled with flow acceleration for spatial and temporal growth of boundary layer. The longitudinal velocity distribution developed from the inlet to section $\phi = 113^\circ$ shows higher velocity occurred along the inner bend. The growth of tubular boundary layer is associated with a transient irrotational core. Similar phenomena appear in the upstream and downstream sections for spatial growth of boundary layer in early systole. The pressure distribution at the section shows higher pressure near the outer bend due to centrifugal forces. The effect is visible in pressure distribution on the longitudinal mid plane. The results indicate a rapid rising of pressure at $t = 0.18$ second with the predominant pressure drops toward the downstream. They are associated with acceleration during early systole. The pressure distribution on the symmetric plane for the peak flow at $t = 0.26$ second with Re reaching 12097 indicates insignificant longitudinal pressure gradients because of dV_o/dt vanished momentarily. At this instant, the presence of radial pressure variations along the curved segment is due to strong centrifugal forces. The w -contour becomes complicated along the inner bend characterized by a hump (refer to $w = 75$ cm/sec) with a pair of peak velocities (see $w = 140$ and 143.4 cm/sec) by its sides. The growth of three-dimensional boundary layers is associated with the secondary flow and pressure variations on the section. The pulsating flow continues with a rapid deceleration.

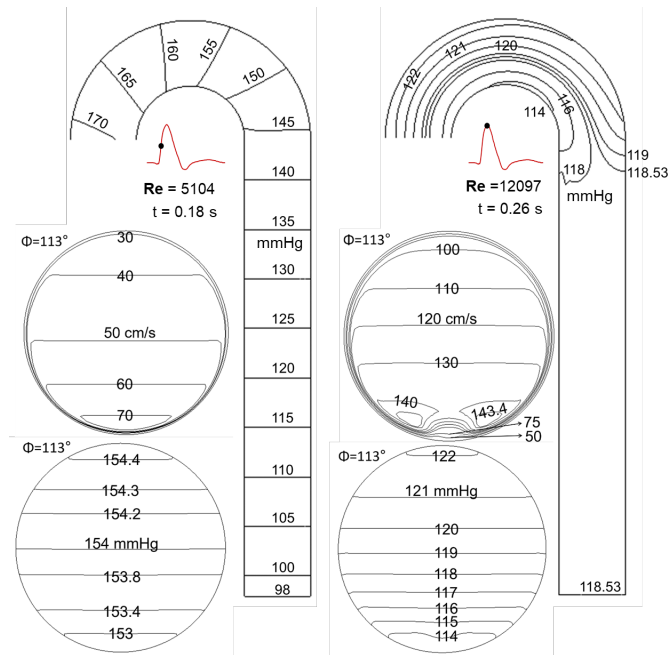


Figure 2: Longitudinal velocity (w) and pressure contours at section $\phi = 113^\circ$ on the symmetric plane for $Re = 5104$ and 12097

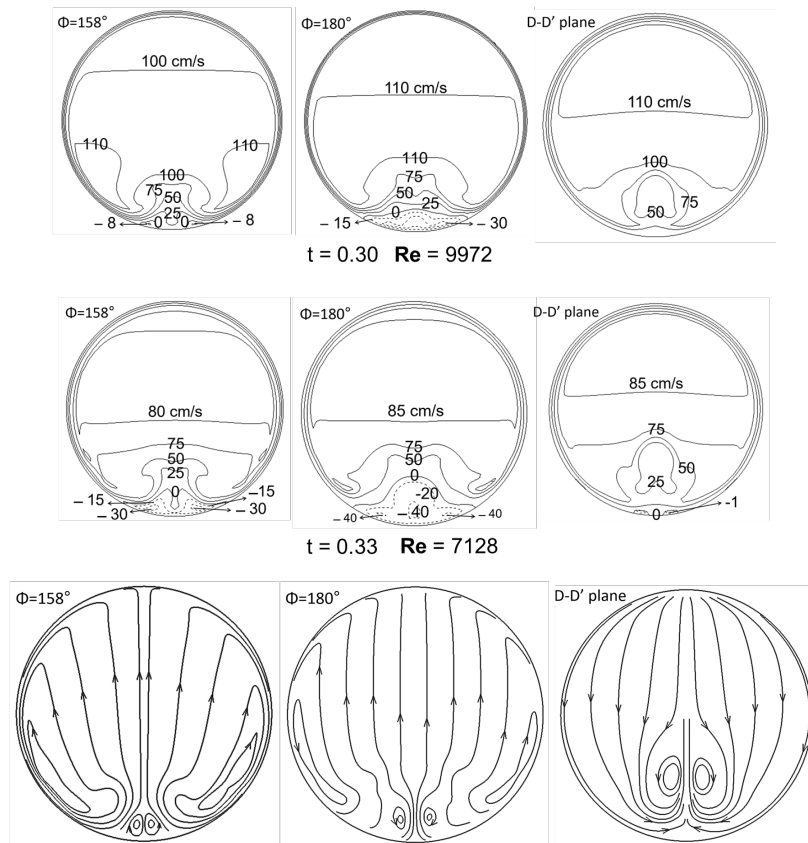


Figure 3: The longitudinal velocity contours and secondary flow patterns

The w -contours at sections $\phi = 158^\circ$ and 180° shown in Fig. 3 depict the development of flow separation when Re is reduced to 9972 at $t = 0.30$ sec. The reversed flow at $\phi = 180^\circ$ is indicated by dashed line for $w = -15$ and -30 cm/sec. The vortex grows rapidly as the flow being decelerated to $Re = 7128$ at $t = 0.33$ sec. The secondary flow patterns on these two sections are also shown in the figure along with the longitudinal velocity distribution on section D-D' which is at one diameter from section $\phi = 180^\circ$.

Further development of laminar layer is demonstrated in Fig. 4 for flow when Re reduces to 5482. For the 3D pulsating flow, the surface of flow separation is not obtainable from stream surfaces [3]. Using the contour of $w = 0$ to demarcate backflow from forward stream is good for analyzing the 3D vortex. Also shown in Fig. 4 is the w -contour and pressure distribution for back flow when $Re = -2132$. The negative velocity (see $w = -60$ cm/sec) on the inner bend is in the laminar layer while the forward momentums remain on the outer bend.

Fig. 5 compares the numerical solutions of w -contour at section $\phi = 135^\circ$ for 5 cycles of computation. The results of the 2nd cycle is between the 1st and 3rd cycles. The first cycle is based on hydrostatic condition when $t = 0$. The results shown in Figs. 2 to 4 are from the solution of the first cycle. They are symmetric from the longitudinal mid-section. The small deviation at the 4th cycle shown in Fig. 5 is due to numerical noise. Because the pulsating flow is dominated by strong systolic acceleration with a prolonged diastole, the computation for several cycles is not necessary for similar endeavors. In fact, cardiac pumping is not rigorously periodic. Thus, using the hydrostatic as the initial condition is practical for CFD analysis. The study does not include the branching flow nor the tapering and twisting of the aortic arch when focusing on the combined effects of curvature and flow pulsation.

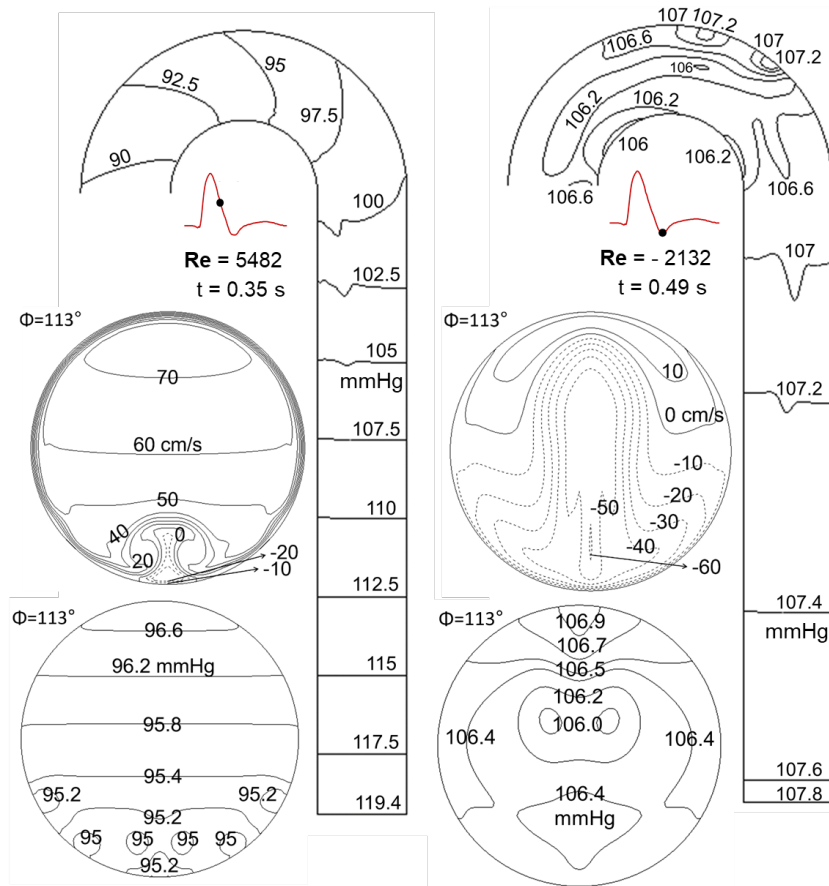


Figure 4: Longitudinal velocity (w) and pressure contours at section $\phi = 113^\circ$ on the symmetric plane for $Re = 5482$ and -2132

4 Concluding Remarks

Development of 3D pulsating blood flow is obtained and analyzed in details by CFD computation. High velocities on the inner bend during systolic acceleration are due to irrotational core. Higher momentums coupled with secondary flow move towards outer bend during systolic deceleration. The symmetry of the computational model is effective for identifying the convergence and validity of the numerical solutions which are confirmed by constancy of flow rate across each section. The transient 3D vortex can be effectively studied in details from the longitudinal velocity contours, the secondary flow patterns and pressure distribution. Otherwise, the enormous detailed results are difficult to present and discuss.

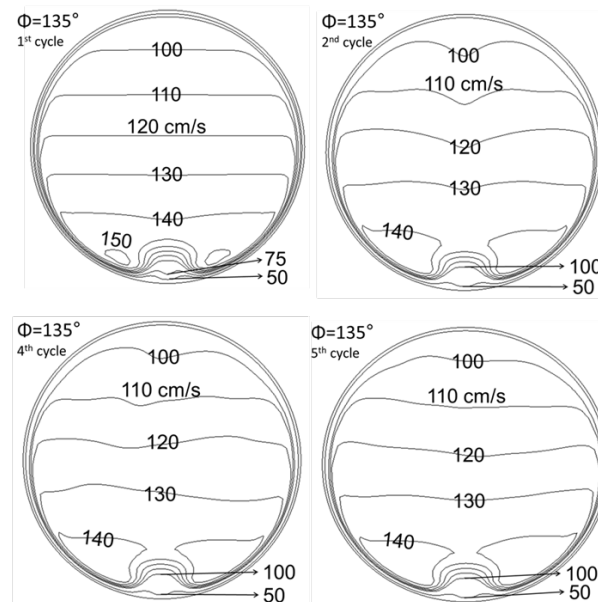


Figure 5: Comparison of the w-contours among different cycles of computation

TKH first met Professor Fung at the 1970 Urodynamics Symposium where he presented a generalized Bernoulli’s equation with energy pumped from the ureter to urine bolus transport [4]. One professor from aerospace engineering made a comment: “I hate to attack a junior colleague. On God’s green world, there is no such Bernoulli equation”. At the conclusion of the conference, Prof. Fung was asked by Dr. Saul Boyarsky for a comment. He said:

“...We are from the conventional engineering fields to work on unconventional biological system. Dr. Hung’s Bernoulli equation was correct.”

This junior colleague, TKH, would later have the honor and opportunity to participate in many activities with Professor Fung, including ASME, ASCE, USNBC, ICMMB, JMMB, and NCKU. His admiration of Dr. Fung’s kindness and friendship is evident in celebrating Professor Fung’s 65th, 90th and 100th birthday conferences at UCSD. This paper is dedicated to Professor Yuan-Cheng Fung for his creativity and leadership in modern biomechanics and biomedical engineering.

Acknowledgement: The fellowships of the Ministry of Education of the Republic of China (Taiwan) from the Medical Device Innovation Centre of the National Cheng Kung University, Tainan, for Rui-Hung Kao and Cheng-Hsien Chiang visiting the University of Pittsburgh are acknowledged. The study is accomplished through the NCKU-Pitt initiative of Professor Fong-Chin Su of NCKU and Professor Tin-Kan Hung of Pitt.

References

1. Fung YC. Biomechanics: Circulation. Springer. **1997**.
2. Hirt CW, Amesden AA, Cook JL. An arbitrary Lagrangian-Eulerian computing method for all flow speeds. *Journal of Computational Physics* **1974**, 14(3): 227-253.
3. Rouse H. Advanced Mechanics of Fluid. John Wiley & Sons. **1963**.
4. Hung TK, Bugliarello G. Information theory and the ureter: from a hydrodynamic point of view. In: Saul Boyarsky et al. (eds.), *Urodynamics*, pp. 486-492. Academic Press, N. Y. **1971**.